POSTER SESSION #4—PERFUSION AND CIRCULATORY ASSISTANCE TECHNIQUES

Recent Progress in Engineering the Pittsburgh Intravenous Membrane Oxygenator

WILLIAM J. FEDERSPIEL,*†‡§ TODD HEWITT,§ MARIAH S. HOUT,§ FRANK R. WALTERS,* LAURA W. LUND,§ PATRICIA J. SAWZIK,* GARY REEDER,* HARVEY S. BOROVETZ,*†‡§ AND BRACK G. HATTLER*†

The University of Pittsburgh intravenous membrane oxygenator (IMO) is undergoing additional engineering development and characterization. The focus of these efforts is an IMO device that can supply as much as one-half basal O_2 consumption and CO_2 elimination rates while residing within the inferior and superior vena cavae after peripheral venous insertion. The current IMO design consists of a bundle of hollow fiber membranes potted to manifolds at each end, with an intra-aortic type balloon integrally situated within the fiber bundle. Pulsation of the balloon using helium gas and a balloon pump console promotes fluid and fiber motion and enhances gas exchange. During the past year, more than 15 IMO prototypes have been fabricated and extensively bench tested to characterize O_2 gas exchange capacity, balloon inflation/deflation over relevant frequency ranges, and the pneumatics of the sweep gas pathway through the device. The testing has led to several engineering changes, including redesign of the helium and sweep gas pathways within the IMO device. As a result, the maximum rate of balloon pulsation has increased substantially above the previous 70 bpm to 160 bpm, and the vacuum pressure required for sufficient sweep gas flow has been reduced. The recent IMO prototypes have demonstrated an O_2 exchange capacity of as much as 90 ml/min/m^2 in water, which appears within 70% of our design goal when extrapolated to scaled up devices in blood. *ASAIO Journal* 1996;42:M435–M442.

Patients with adult respiratory distress syndrome (ARDS) need temporary respiratory support until their lungs return to normal gas exchange function. The preferred method of treatment in ARDS is mechanical ventilation with high inspired O_2 levels. However, the positive lung airway pressures and excessive volumes associated with ventilation can lead to barotrauma, volutrauma, and impairment of cardiovascular function, resulting in an overall worsening of the state of the ARDS lung and the health of the patient.[1] Respiratory support also can be accomplished with extracorporeal oxygenation (ECMO), but ECMO is labor intensive, expensive, and subject to complications and mechanical failure of the extracorporeal pumping circuit.[2] Thus, a clear clinical need exists for a respiratory support device that is simple, economic, and effective.

Intravenous oxygenation is a potentially attractive therapy for respiratory support in patients with ARDS. An intravenous oxygenator consists of a long, slender bundle of hollow fiber membranes (manifolded to gas supply and removal lines) that can be placed within the vena caval system through insertion at a peripheral vein site. The only intravenous oxygenator that has progressed to clinical testing has been the IVOX device developed by Mortensen.[3] The IVOX used kinked hollow fiber membranes in bundles with surface areas from 0.2 to 0.5 m^2, and accomplished levels of gas exchange averaging as much as 30% of metabolic requirements in patients with ARDS.[4] Although the devices were implanted for as long as 29 days, with no marked degradation in device gas exchange and with no serious complications from thromboembolism, the multicenter clinical trial indicated that greater gas exchange, approaching 50% of metabolic requirements, would make the oxygenator more clinically efficacious. However, simply increasing the membrane surface area to increase intravenous gas exchange would most likely compromise venous hemodynamics and restrict cardiac return.

Our development efforts in intravenous oxygenation have focused on increasing the efficiency of gas exchange (the gas exchange per membrane area) by using a pulsating balloon within the fiber bundle to actively promote fluid mixing and augment gas exchange.[5] Our intravenous membrane oxygenator (IMO) has demonstrated significant gas exchange enhancement with balloon pulsation. Additional progress in developing the IMO requires not only optimizing balloon augmentation of gas exchange but also examining all aspects of device performance affecting gas exchange. Our engineering focus is on identifying, then modifying or eliminating, factors that can limit gas exchange in intravenous oxygenators. Specifically, this report describes studies and improvements in balloon pulsation function, gas flow within our device, and gas exchange performance *in vitro*. The results of *in vivo* testing are described in an accompanying report.[6]

IMO Prototype Description

The current IMO prototype (Prototype D Series), shown schematically in **Figure 1**, incorporates a centrally positioned elongated balloon (analogous to the intra-aortic balloon)

From the *Artificial Lung Program, †Department of Surgery, ‡Department of Chemical Engineering, and the §Bioengineering Program, University of Pittsburgh, Pittsburgh, Pennsylvania.

Reprints requests: William J. Federspiel, PhD, Artificial Lung Program, University of Pittsburgh, Room 428, Biotechnology Center, 300 Technology Drive, Pittsburgh, PA 15219.

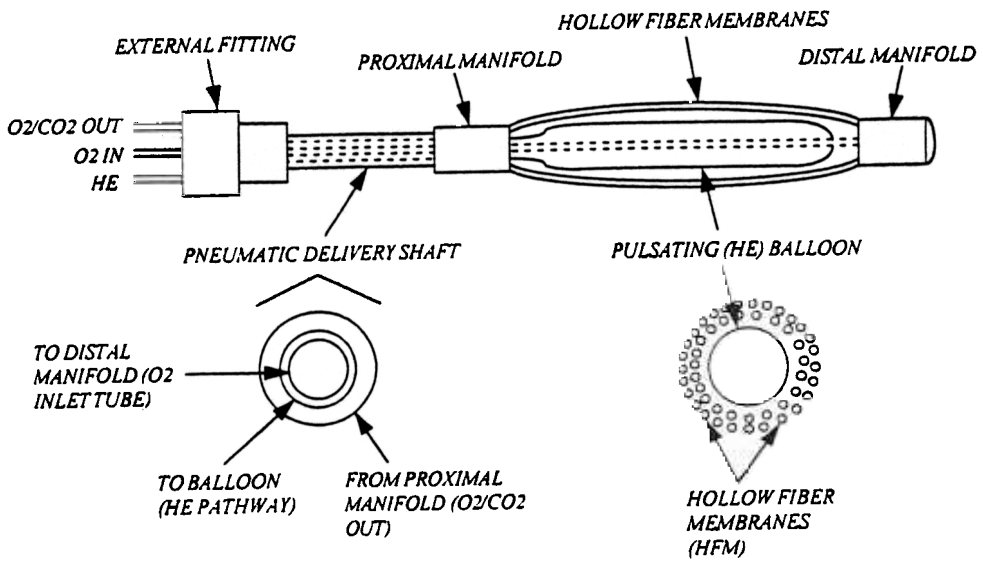

Figure 1. Schematic of the IMO prototype D series incorporating a central polyurethane balloon within a hollow fiber membrane bundle. An integral, implantable size pneumatic delivery shaft accommodates the inlet and outlet gas pathways and the helium pathway for balloon activation.

within the fiber membrane bundle. Gas pathways for O_2 supply, CO_2 removal, and helium pulsation to the balloon run concentrically through a pneumatic delivery shaft extending from an external fitting to the proximal fiber bundle manifold (the length of the pneumatic delivery shaft can be tailored to insertion requirements). The O_2 supply pathway, which operates under vacuum pressure, continues past the proximal manifold and through the balloon center to supply sweep gas to the distal manifold. The helium gas used to pulsate (inflate/deflate) the central balloon is driven by a Datascope 90 (Paramus, NJ) intra-aortic balloon pump console. The prototypes studied here were scaled down devices with respect to fiber bundle length, but full-size devices with respect to fiber bundle girth, which was selected as the maximal size compatible with peripheral venous insertion. The number of fibers within the IMO device varied from approximately 700 to 1,100, depending on fiber size, and the corresponding aggregate membrane areas spanned from 0.13 to 0.16 m^2 for the scaled down bundle lengths of 20 cm.

Although the IMO development program has evolved through six different device configurations (Prototypes A through F) with the best *in vitro* gas exchange performance in the Prototype F series[5] (a scrolled mat of hollow fiber membranes arranged with the fiber axis perpendicular to the flow of blood), the dense fiber mats of Prototype F presented an appreciable flow resistance and substantial difficulties with peripheral venous insertion. As a result, current IMO efforts have focused on additional development of the simpler Prototype D device, which presents a markedly smaller resistance to flow per fiber area and is more readily insertable at peripheral vein sites. The IMO Prototype D series was modified to incorporate the gas inlet and outlet pathways and the helium pathway into a integral, implantable size pneumatic delivery shaft.

IMO Balloon Pulsation Dynamics

Balloon pulsation enhances IMO gas exchange by increasing fluid convection past and through the fiber bundle, thereby reducing the diffusional boundary layer resistance at the fiber surface. The additional convective flow generated by the balloon depends on the volume amplitude of balloon filling and the frequency of pulsation. However, in past studies the enhancement of gas exchange reached a maximum (then decreased) as balloon pulsation increased beyond 60-80 bpm.[5] This behavior suggests a diminution in balloon (stroke) volume as pulsation frequency increases. As frequency increases, effective balloon pulsations (pulsations that can completely inflate/deflate the balloon) can diminish because the time available for inflating/deflating the balloon decreases, whereas shuttling helium through the device requires a finite time, depending on the pneumatic impedance of the helium pathway. Thus, a maximum or "critical" frequency exists beyond which the balloon cannot fill and empty completely and thus cannot pulsate effectively. As part of development efforts toward improving gas exchange performance, we studied the balloon pulsation dynamics in IMO prototype devices.

Balloon Pulsation "Frequency Spectrum"

The critical pulsation frequency of an IMO prototype can be determined from its "frequency spectrum," the volume amplitude of balloon pulsation at different frequencies. Balloon frequency spectrums were determined plethysmographically by placing the IMO device in an airtight, water filled chamber with a small volume of trapped air. The pressure swings associated with balloon inflation/deflation within the box were measured and converted to volume changes using the ideal gas law. The volume of trapped air was adjusted such that the maximum pressure never exceeded 30 mmHg above atmospheric, so the back pressure counteracting balloon inflation was kept relatively small.

The balloon inflation/deflation volume amplitudes were measured over a range of pulsation frequencies in an IMO D series device (Prototype D03, **Figure 2A.**) The critical frequency was defined as the frequency at which the balloon pulsation volume amplitude decreased to 95% of balloon

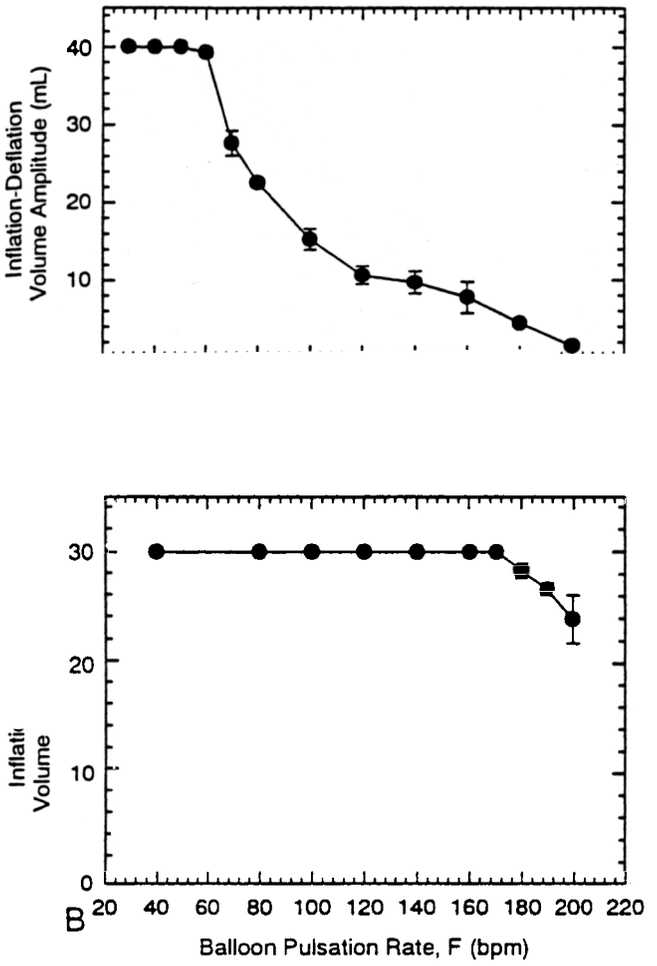

Figure 2. Volume amplitude of balloon filling and emptying over a range of pulsation frequencies (the balloon pulsation frequency spectrum). **(A)** Prototype D03: before redesign of the helium pathway. **(B)** Prototype D08.1: after modification and redesign of the helium pathway.

volume and is approximately 60 bpm for the device shown. Beyond approximately 100 bpm, the balloon pulsation volume drops to less than 1/4 of the balloon volume. Note that the frequency spectrum shows only the inflation/deflation amplitude, and thus does not reveal whether the balloon is failing in an inflated or deflated state.

Modification of Helium Pathway

The critical frequency of an IMO prototype reflects limitations in shuttling helium volumes because of the pneumatic impedance of the helium pathway within the device. The helium pathway is an annular pathway, concentric with the oxygen inlet pathway, that runs through the integral pneumatic delivery shaft **(Figure 1).** The impedance of the helium pathway can be decreased by increasing the helium pathway size. Because the radius of the oxygen inlet tube plus the thickness of the helium gap must remain fixed (so that the overall size of the pneumatic delivery shaft is kept minimal), increasing the helium pathway size requires decreasing the oxygen inlet tube size.

The predicted tradeoff between increasing the critical frequency and maintaining a sufficient oxygen flow rate (for a given pressure drop in the sweep gas pathway) is explored in **Figure 3** as a function of the diameter of the oxygen inlet tube. The results shown are based on appropriate viscous flow modeling of oscillating flow in the helium pathway and steady flow through the O_2 inlet tube. The principal result is that the critical frequency, f_{crit}, can be considerably increased by only a small decrease in the size of the O_2 inlet tube and thus with only a small effect on the oxygen flow through the inlet tube for a given pressure drop. For example, reducing the O_2 inlet tube inner diameter from 0.124 to 0.112 inches increases the critical frequency from 50 to 200 bpm but reduces O_2 flow rate by less than 1%.

The design constraints embodied in **Figure 3** were used to modify the helium pathway within the IMO D series device. The balloon pulsation frequency spectrum for the modified IMO device (Prototype D08 series) is shown in **Figure 2B.** The critical frequency of the modified IMO devices is greater than 160 bpm, which represents approximately a threefold improvement in helium balloon pulsation compared with that of the premodified D prototypes **(Figure 2A).** In addition, the oxygen flow rate per given pressure drop through the sweep gas pathway essentially was unaffected. The helium pathway could be modified more to increase pulsation rates, but limitations associated with the helium drive console and *in vivo* constraints ultimately may set an upper limit on pulsation frequency.

Flow Dynamics of the Sweep Gas Pathway

The flow dynamics of the sweep gas pathway affect the exchange of both O_2 and CO_2. The principle driving force for exchange is the difference between the partial pressure

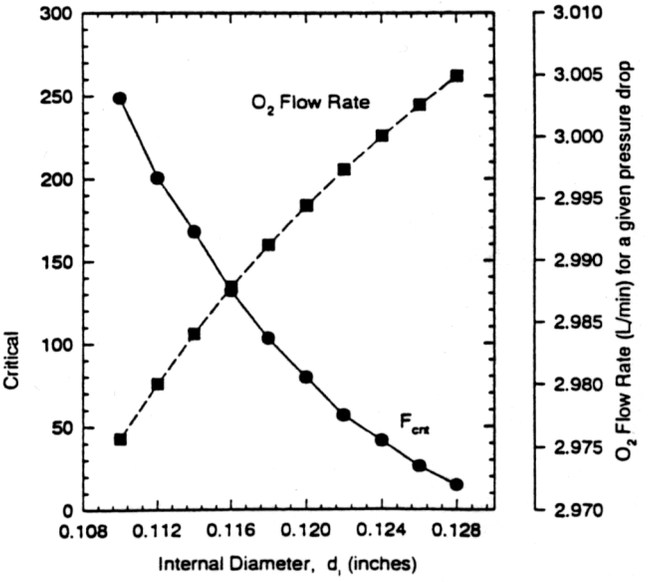

Figure 3. Predicted tradeoff between increased helium pathway dimensions and decreased oxygen inlet tube size. The diameter shown represents the outer diameter of the oxygen inlet tube and the inner diameter of the helium pathway.

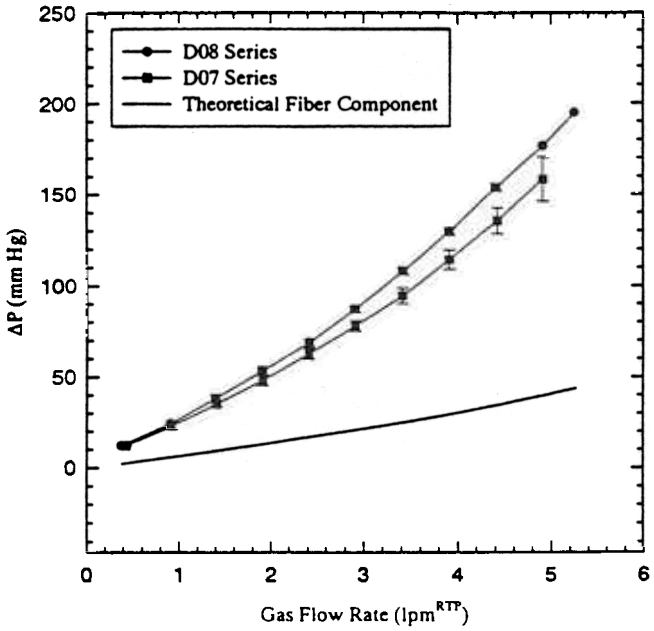

Figure 4. Pressure drop-flow rate relationship in IMO series D prototypes (D07 and D08).

in the sweep gas and that in the liquid. In the IMO device, the sweep gas flows under vacuum pressure, the level of which depends upon pressure losses incurred throughout the gas pathway. For O_2, gas-side concentration is nearly 100% and O_2 partial pressure is approximately equal to total pressure, so maintaining a maximal gas-liquid PO_2 gradient requires minimal pressure losses in the prefiber gas pathway. For CO_2, maintaining a maximal gas-liquid PCO_2 gradient requires a sufficiently high flow rate of sweep gas, so that CO_2 does not accumulate in the fibers and the PCO_2 can be kept near zero. Thus, effective transfer of both O_2 and CO_2 requires a sweep gas pathway with minimal pressure drops at flow rates of 3 to 6 L/min. As part of development efforts toward improving gas exchange performance, we studied the pressure-flow rate relationship in the sweep gas pathway of our IMO devices.

Measurement of Pressure Drop-Flow Rate Relationship

Pressure drop-flow rate studies were done on seven IMO D series devices. Four devices were from the D07 series used in acute *in vivo* testing[6] and contained 720 fibers with 0.025 cm inner diameter and 20 cm long. Two devices were from the D08 series with the modified helium pathway. These devices had identical fiber bundles to those of the D07 series but had oxygen inlet tubes of reduced diameter in accordance with the modified helium pathway. One device from the D02 series also was used that contained 960 fibers of 0.02 cm inner diameter and 37 cm length. This device was fitted with additional pressure taps at the inlet and outlet manifolds to provide greater resolution of the pressure distribution within the IMO.

Pressure Distribution in Sweep Gas Pathway

The total pressure drop required to drive vacuum flow through the IMO D07 and D08 series devices in the range from 0 to 5 L/min is shown in **Figure 4.**The smaller O_2 inlet tube in the D08 series leads to a small increase in overall pressure drop compared with that of the D07 series. Gas flow rates of from 3 to 6 L/min are required for maximal CO_2 exchange, so the D07 and D08 series devices would require no more than an approximately 200 mmHg vacuum to operate at these flow rates. Even if the entire pressure loss oc-

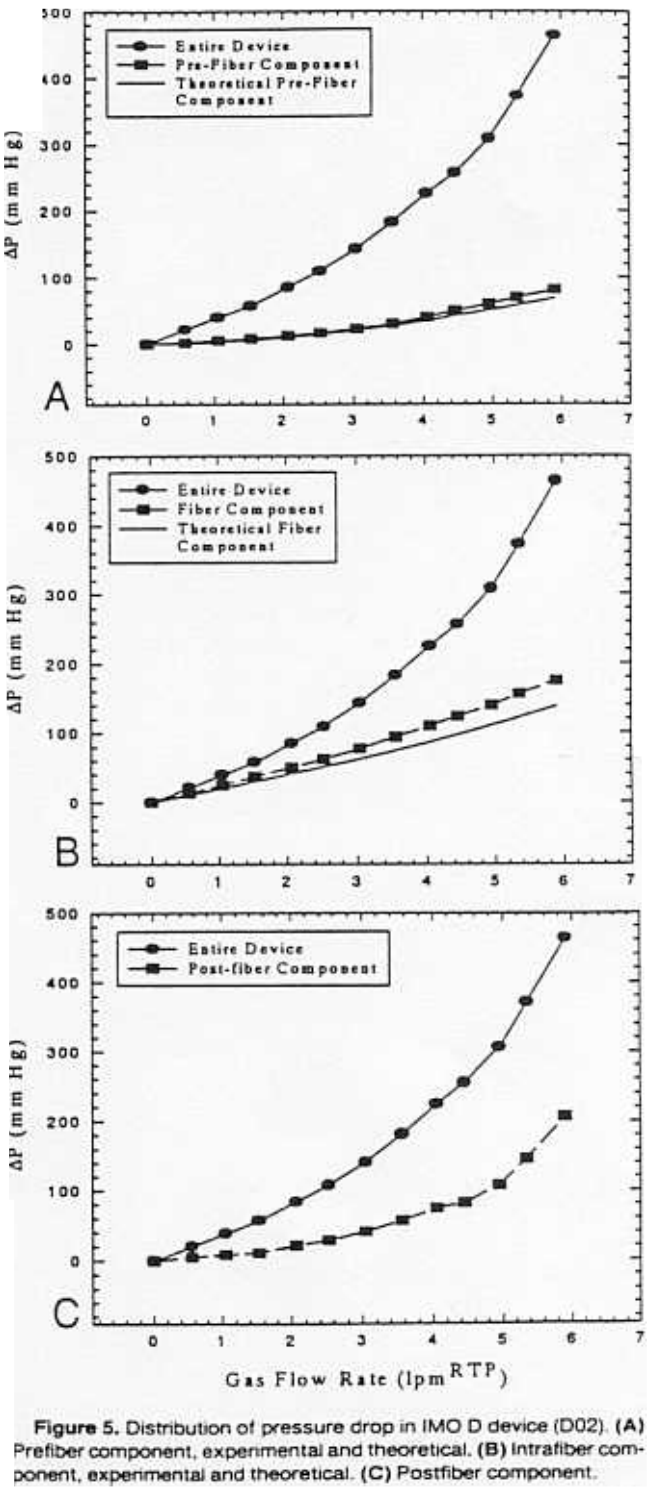

Figure 5. Distribution of pressure drop in IMO D device (D02). **(A)** Prefiber component, experimental and theoretical. **(B)** Intrafiber component, experimental and theoretical. **(C)** Postfiber component.

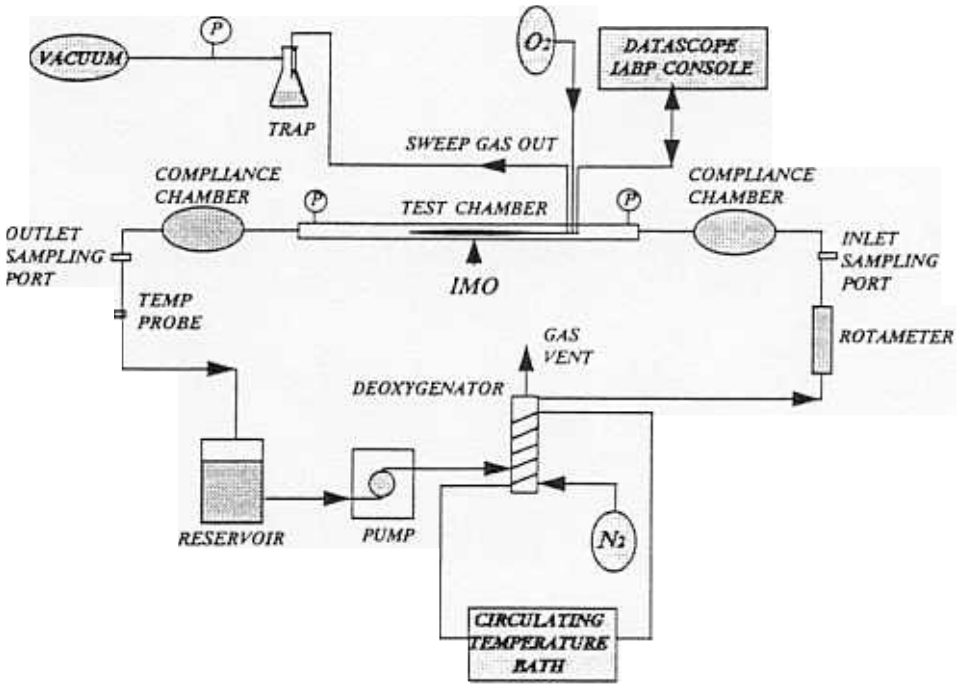

Figure 6. The *in vitro* bench test system used for gas exchange performance studies of IMO prototypes.

curred before the fiber bundle, the PO_2 in the fibers and, consequently, the driving force for O_2 exchange would be reduced by only 25% as a result of pressure losses.

Gas flow through the fiber bundle obeys compressible Poiseuille theory:[7]

$$P_o^2 - P_i^2 = 2RP_{atm}Q \quad (1)$$

where P_0 and P_i are the pressures at the fiber ends, $R = 128 \mu l/N \pi D^4$ is the Poiseuille flow resistance (N, number of fibers; μ, gas viscosity; l, fiber length; and D, fiber diameter), and Q is the gas flow rate. Thus, the pressure drop attributable to the fiber bundle can be estimated and compared with the overall pressure drops shown in **Figure 4** (fiber pressure drop is solid line in the figure). Most of the pressure drop in these IMO devices occurs outside the fiber bundle. Scaling up the membrane surface area of an IMO device by increasing the length of the fiber bundle may have a only small impact on the overall pressure drop through the device.

The serial distribution of pressure losses through the IMO device also was studied by incorporating additional pressure taps at the inlet and outlet manifolds of an older IMO device (D02 series), and the results are shown in **Figure 5A–C.** Note

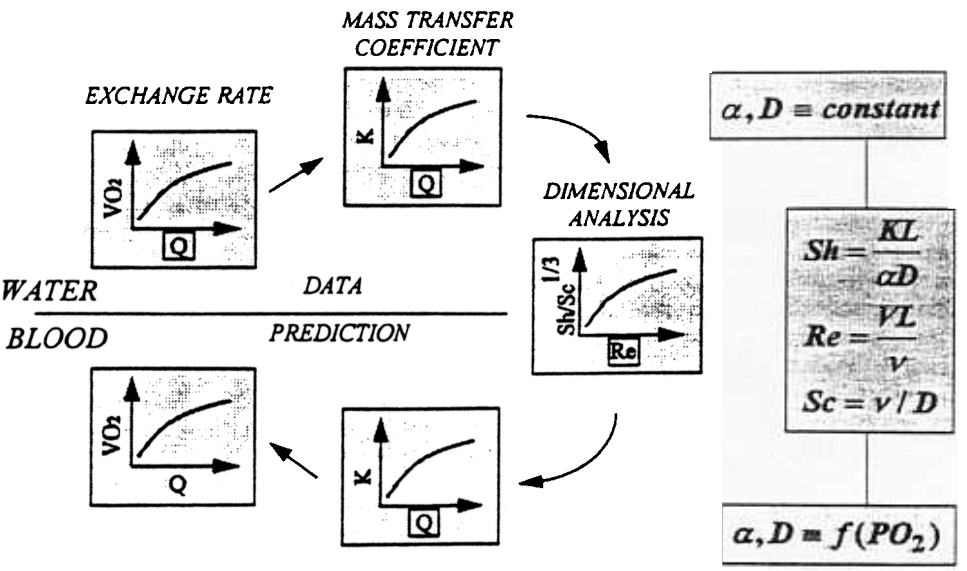

Figure 7. Data analysis methods for estimating O_2 exchange in blood from measurements of O_2 exchange in water.

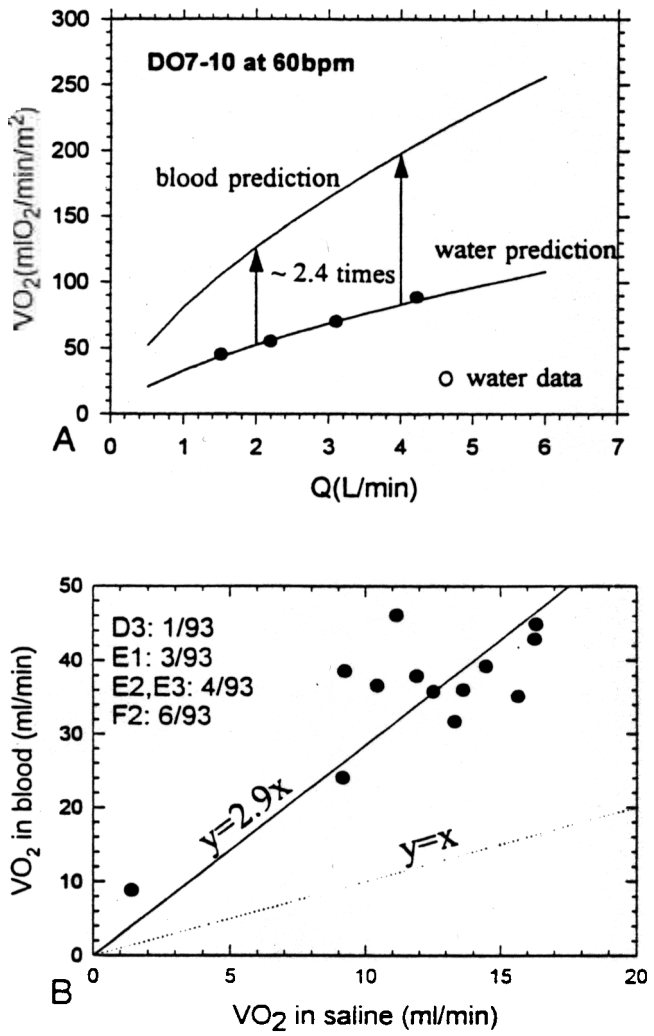

Figure 8. O_2 exchange of IMO prototypes in blood *vs* in water. **(A)** O_2 exchange estimated in blood from that measured in water. **(B)** Experimental measurements of O_2 exchange in blood *vs* saline from past IMO prototypes.

that the total pressure drop through this device (approximately 400 mmHg at 5 L/min^{RTP}) is higher than that of the D07 and D08 series prototypes (**Figure 4**) because the smaller diameter fibers of the D02 device increase the resistance of its fiber bundle threefold compared with those of the D07 and D08 series devices. Distribution of the total pressure drop among prefiber, intrafiber, and postfiber components of the IMO device is shown in **Figure 5A–C,** respectively. The prefiber component of the pressure drop (**Figure 5A**) is small and agrees well with predictions based on flow through the O_2 inlet tube, which suggest that the pressure drop in the inlet manifold is minimal. The fiber component of the total pressure drop (**Figure 5B**) accounts for nearly half of the flow resistance. The experimental results are slightly higher than those predicted for compressible Poiseuille flow through the fiber bundle. The postfiber component of the pressure loss (**Figure 5C**) also accounts for a large percentage of the total pressure drop. Although it has no effect on the mass transfer capabilities of the device, it may be desirable to redesign this part of the pathway to reduce the power needed to pump the sweep gas.

Gas Exchange Performance Testing

The IMO design evaluation and evolution process requires that extensive gas exchange performance studies be readily and repeatably made in an *in vitro* bench test system. The IMO prototypes are bench tested in the perfusion loop shown in **Figure 6.** The loop consists principally of a vena cava test section (a 1 inch inner diameter Plexiglas tube) within which the IMO device is placed, a centrifugal pump for providing steady flow rates, an extracorporeal oxygenator module used as a deoxygenator and heat exchanger, compliance chambers for damping fluid pressure oscillations engendered by balloon pulsation, liquid sampling ports for measuring PO_2 in the water before and after the test section, and gas and liquid side flow meters and pressure taps. The IMO device is placed within the test section, which is perfused with from 1 to 6 L/min of distilled water at 37°C. Pure O_2 sweep gas is run through the IMO device under vacuum at 3 L/min. The rate of O_2 exchange is computed from the product of the PO_2 difference in water across the test section, water flow rate, and the solubility of O_2 in water. At a given water flow rate, the O_2 exchange rate (VO_2) is measured over a range of balloon pulsation rates to 160 bpm, depending on the prototype. At a given flow rate through the test section and a given balloon pulsation rate, exchange measurements are made with the prototype in angular orientations of 0, 120, and 240 degrees of rotation.

Estimating Gas Exchange in Blood

A dimensionless analysis of the *in vitro* O_2 exchange data in water is used to estimate exchange performance for bench testing in blood under physiologic flow conditions. The overall procedure is illustrated in **Figure 7** and is adopted from that developed and evaluated by Vaslef *et al.*[8] for extracor-

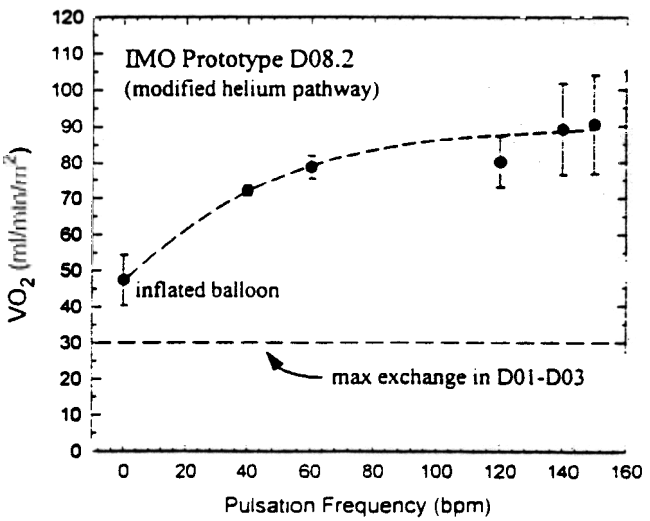

Figure 9. Gas exchange performance of recent IMO prototype with modified helium pathway determined from *in vitro* testing in water.

poreal artificial lungs. At a given pulsation rate, the exchange rate (VO_2) is determined over the relevant flow rate range (Q). The exchange rate is recast as a device mass transfer coefficient (K), which represents the exchange rate per unit area and unit partial pressure difference between gas and liquid phases. The dimensionless form of the K, Q relationship is $Sh/Sc^{1/3}$ *vs* Re, for which Sh, Sc, and Re are the Sherwood, Schmidt, and Reynolds numbers, respectively, as defined in **Figure 7.** The dimensionless form is fluid invariant (applies to blood and water equally) because the oxygen solubility and diffusiveness in the liquid, α and D, respectively, and the liquid kinematic viscosity, ν, are used in the scaling. Accordingly, the dimensionless relationship can be recast into a K, Q form for blood, provided α and D account for O_2 binding to hemoglobin in blood,[8] so the VO_2 *vs* Q relationship for blood can be computed. Estimating the exchange performance in blood from water testing is important because a given prototype exchanges more gas in blood than in water under equivalent conditions. Because water testing is simpler and more expedient, the development time and effort associated with design evaluation, design change/adjustment, and design re-evaluation are shortened.

The estimation of O_2 exchange rate in blood from water testing is evaluated in **Figure 8.** In **Figure 8A** the symbols represent the measured O_2 exchange rate in water flowing from 1 to 5 L/min. This data underwent the dimensionless analysis illustrated in **Figure 7,** and the predicted exchange rate in blood (for standard Association for Advancement of Medical Instrumentation conditions) is shown in **Figure 8A** as the solid line (blood prediction). The analysis for this IMO prototype indicates an exchange rate in blood that is 2.4 times greater than that in water. In general, all IMO prototypes that have been tested and analyzed in this manner suggest a broader range of twofold to threefold greater O_2 exchange rate in blood than in water. In **Figure 8B,** all available data for the O_2 exchange rates of IMO prototypes tested in blood are compared with their respective O_2 exchange rates in saline under (otherwise) equivalent conditions. The average ratio of O_2 exchange in blood *vs* water indicated by the ensemble experimental data is 2.9, a ratio consistent with the specific IMO predictions shown in **Figure 8A.**

Gas Exchange Performance in Modified IMO

Past performance data for gas exchange in IMO prototypes has indicated a maximal exchange rate with balloon pulsation rates of 60–80 bpm, with a decrease in gas exchange at higher pulsation frequencies.[5] The first IMO D series prototypes (Prototypes DO1–D03) with the implantable size, integrated pneumatic delivery shaft **(Figure 1)** for sweep gas inflow and outflow and for helium delivery to the balloon could pulsate effectively only to approximately 60 bpm **(Figure 2A)** because of the pneumatic impedance of the helium pathway within the device, as described. However, the helium pathway was redesigned to reduce its pneumatic impedance, and the resulting IMO prototypes (Prototypes D08 and higher) could pulsate effectively to 150–160 bpm **(Figure 2B).** These modified prototypes underwent gas exchange testing *in vitro* (in water) to determine the degree to which improvements in balloon pulsation translated to better O_2 exchange performance.

The O_2 exchange rate as a function of the balloon pulsation frequency for a modified IMO prototype (D08.2) is shown in **Figure 9.** With no balloon pulsation (but with the balloon inflated), the O_2 exchange was approximately 45 ml/min/m^2 in water. With increasing frequency of balloon pulsation, the O_2 exchange rate continually increased to 150 bpm, the highest beat rate tested. The maximal O_2 exchange rate was 90 ml/min/m^2 at the highest beat rate, which represents a doubling of gas exchange compared with no pulsation (with the balloon inflated). Thus, modifications to the helium pathway eliminated the drop in gas exchange that occurred above 60–80 bpm and was associated with balloon failing in earlier prototypes.[5] Nevertheless, although the balloons in these prototypes can pulsate effectively to 150 bpm **(Figure 2B),** the O_2 exchange rate essentially reaches a plateau with increasing frequency above 80 bpm, and there appears only a modest additional gain in gas exchange to the maximum frequency of 150 bpm. Because the balloon is able to fill and empty completely, the convective flow generated by the balloon at 150 bpm is nearly double that at 80 bpm, yet this additional convective energy appears to have a relatively small additional effect on reducing mass transfer resistance. The nature of this behavior is unclear, and additional work is being done to delineate its contributing mechanisms.

Summary

Additional developmental work on the Pittsburgh intravenous membrane oxygenator (IMO) has focused on the Prototype D series device, which presents a smaller resistance to flow and is more readily insertable than are other prototypes examined previously.[5] The gas inlet and outlet pathways and the helium pathway for balloon activation have been incorporated into an integral, implantable size pneumatic delivery shaft. Redesign of the helium pathway in the IMO has increased the maximal balloon pulsation rate from 60 bpm to more than 150 bpm. Sweep gas flows as great as 5 L/min through the device can be driven by a smaller than 300 mmHg vacuum. The current IMO prototypes can exchange as much as 90 ml O_2/min/m^2 in bench testing with water, which corresponds to an estimated O_2 exchange rate in blood of approximately 200 ml/min/m^2 under equivalent conditions. This level of exchange appears within 70% of our design goal, and additional work will address the optimization of gas exchange enhancement with balloon pulsation, which currently tends to plateau beyond pulsation rates of 80 bpm, despite full balloon inflation and deflation.

We believe that a clinically efficacious intravenous oxygenator (as well as other intracorporeal oxygenators) can be developed by increasing the efficiency of gas transfer at the fiber level to overcome limitations in implantable membrane surface area. In this regard, a mechanism for enhancing convective mixing and instilling additional energy into the vena caval system most likely will be a key component of future intravenous oxygenators.

Acknowledgments

This work was supported by the United States Army Medical Research, Development, Acquisition, and Logistics Command under Contract No. DAMD17-94-C-4052. Also supported by Medtronic Inc. and the McGowan Foundation.

The views, opinions, or findings contained in this report are those of the authors and should not be construed as an official Department of the Army position, policy, or decision unless so designated by other documentation.

References

1. Weinberger SE: *Principles of Pulmonary Medicine*. Philadelphia, WB Saunders Company, 1992.
2. Fazzalari FL, Bartlett RH, Bonnell MK, Montoya JP:An intrapleural lung prosthesis: rationale, design, and testing. *Artif Organs* 18: 801–805, 1994.
3. Mortensen JD: Intravascular oxygenator: a new alternative method for augmenting blood gas transfer in patients with acute respiratory failure. *Artif Organs* 16: 75–82, 1992.
4. Conrad SA, Bagley A, Bagley B, *et al:* Major findings from the clinical trials of the intravascular oxygenator. *Artif Organs* 18: 846–863, 1994.
5. Hattler BG, Reeder GD, Sawzik PJ, *et al:* Development of an intravenous membrane oxygenator: enhanced intravenous gas exchange through convective mixing of blood around hollow fiber membranes. *Artif Organs* 18: 806–812, 1994.
6. Macha M, Federspiel WJ, Lund L, *et al:* Acute in-vivo studies of the Pittsburgh intravenous oxygenator. *ASAIO J.* 42:000–000, 1996.
7. Federspiel WJ, Williams J, Hattler BG: Gas flow dynamics in hollow-fiber membranes. *AIChE J.* [In press.].
8. Vaslef SN, Mockros LF, Anderson RW, Leonard RJ: Use of a mathematical model to predict oxygen transfer rates in hollow fiber membrane oxygenators. *ASAIO J* 40: 990–996, 1994.